

Photoconductivity in relaxation semiconductors including certain amorphous materials

J. F. Schetzina

Department of Physics, North Carolina State University, Raleigh, North Carolina 27650

(Received 7 July 1978)

Analysis of the intrinsic photoconductivity spectrum for a conductivity-locked relaxation semiconductor is presented which provides a basis for extracting transport parameters from photoconductivity and absorption measurements. Decreasing photoconductivity in the strong absorption regime, as is observed for *a*-Si:H films, for example, is a predicted effect resulting from surface recombination.

The recent development of new growth and doping techniques for amorphous semiconductors has led to renewed interest in this class of materials. The hydrogenated semiconductors *a*-Ge:H and *a*-Si:H are cases in point. With hydrogenation, the extended state or bandlike conduction properties of these amorphous systems become directly displayed, and accurate and correct characterization of transport processes is essential if the full potential of these new materials is to be realized. By considering these along with most other amorphous semiconductors to be examples of relaxation semiconductors, we address this problem directly and suggest a new technique for obtaining transport parameters for such materials. A new and fundamentally different interpretation of observed behavior in materials such as *a*-Si:H emerges from the present work.

Fast dielectric relaxation processes provide the basic mechanism for maintaining local charge neutrality in lifetime semiconductors. In relaxation semiconductors,¹⁻⁵ however, dielectric relaxation times are large compared with carrier lifetimes and local charge neutrality is controlled by rapid recombination. This recombination is of a particular type. It is *equality* recombination, or recombination at centers which involves capture of electrons and holes at equal total rates per unit volume. With equality recombination, steady-state photoconductivity in relaxation semiconductors is due mainly to an increase in mobile majority-carrier concentration. This is in contrast to the trap-free lifetime case, in which photoexcitation produces an excess carrier plasma consisting of equal densities of electrons and holes.

Recombination in illuminated relaxation semiconductors containing large densities of equality centers gives rise to a linear conductivity-locked mode of transport^{3,4} in which the equilibrium (dark) conductivity ratio is maintained under illumination. In this case, in the absence of an applied magnetic field, the properties of the photo-generated electron-hole plasma are determined by four transport parameters. These are a con-

ductivity-locked diffusion length L^* , surface numbers S_1 and S_2 (defined as the ratio of the carrier recombination velocity to its bulk diffusion velocity) which characterize the plasma-surface interactions, and the equilibrium conductivity ratio $K = \sigma_n / \sigma_p$. This paper elaborates on an earlier analysis³ and suggests a method for obtaining values for all of the above parameters. The method involves measurement of the steady-state photoconductance ΔG and optical absorption coefficient α at selected wavelengths in the strong absorption regime. Measurements of this type are readily obtained using standard experimental techniques and the method, therefore, should be applicable to a wide variety of relaxation-case materials.

We consider here a specimen of the type analyzed in Ref. 3 having a thickness y_0 and unit dimensions along x and z . It is assumed that the surface at $y=0$ is uniformly illuminated with I_0 unreflected photons per unit area, and that the photocurrent flows along x . For this geometry the photoconductance may be expressed as

$$\Delta G = \Delta\sigma [C_1(1 - e^{-Y_0}) + C_2(e^{Y_0} - 1) + (1 - e^{-AY_0})/A], \quad (1)$$

where

$$\Delta\sigma = \frac{(1+K)^2}{2K} \frac{e^2\beta I_0 L^{*2}}{kT} \frac{A}{1-A^2}, \quad (2)$$

$$C_1 = -\frac{(S_1+A)(S_2+1)e^{Y_0} - (S_2-A)(S_1-1)e^{-AY_0}}{2(S_1S_2+1)\sinh Y_0 + 2(S_1+S_2)\cosh Y_0}, \quad (3)$$

$$C_2 = \frac{(S_1+A)(S_2-1)e^{-Y_0} - (S_2-A)(S_1+1)e^{-AY_0}}{2(S_1S_2+1)\sinh Y_0 + 2(S_1+S_2)\cosh Y_0}. \quad (4)$$

In the above expressions β is the quantum efficiency electron-hole pair creation, $A = \alpha L^*$ is a dimensionless absorption coefficient, $Y_0 = y_0/L^*$ is a dimensionless thickness, and S_1 and S_2 are surface numbers for the surfaces at $y=0$ and $y=y_0$, respectively. Other parameters have their usual meanings as defined in Ref. 3.

In Figs. 1-3, plots of ΔG vs- α are shown for specimens of two different thickness and for different combinations of transport parameters as indicated. The solid curves are plots of (1) and have been displaced vertically by various amounts for display purposes. In Fig. 1, photoconductivity spectra for a 1.0- μm -thick film having $S_1=10$ and $S_2=1$ are illustrated. Physically, these surface numbers might apply for a film which has been exposed to ambient impurities such that the recombination velocity for a carrier at the illuminated surface is ten times its diffusion velocity. Note that the photoconductance peaks and then decreases in the strong absorption region in a manner which depends on the magnitude of L^* . Equation (1) predicts a maximum in the photoconductance whenever $S_1 > 0$. *Recombination process at the illuminated surface are thus responsible for the decrease in ΔG at large values of α .* This conclusion is consistent with that of DeVore,⁶ who earlier has presented a single-carrier theory of photoconductivity. The dashed curves in Figs. 1-3 correspond to spectra for $S_1=0$. Figure 2 illustrates the effect of enhanced surface recombination corresponding to $S_1=200$. This gives rise to a larger decrease in photoconductance in the strong absorption regime as indicated. Note also that for $\alpha \gtrsim 2 \times 10^4 \text{ cm}^{-1}$ the photoconductance curves for relatively large diffusion lengths exhibit positive curvature. In contrast to this, the spectrum for $L^*=10^{-6} \text{ cm}$ shows a much broader maximum and negative curvature.

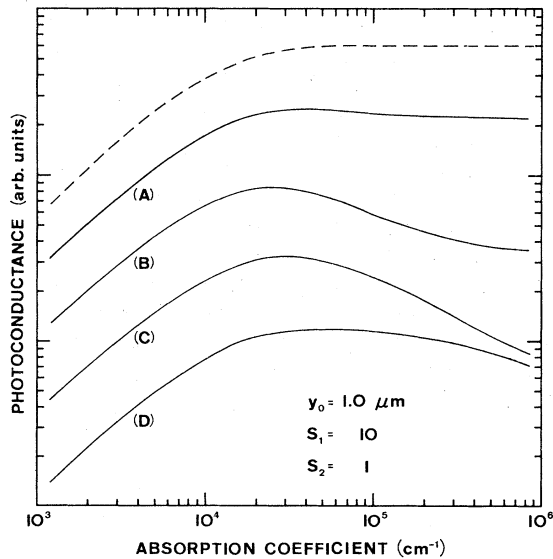


FIG. 1. Photoconductance vs absorption coefficient for 1.0- μm -thick specimen having $S_1=10$, $S_2=1$, and L^* equal to (A) 10^{-3} , (B) 10^{-4} , (C) 10^{-5} , and (D) 10^{-6} cm.

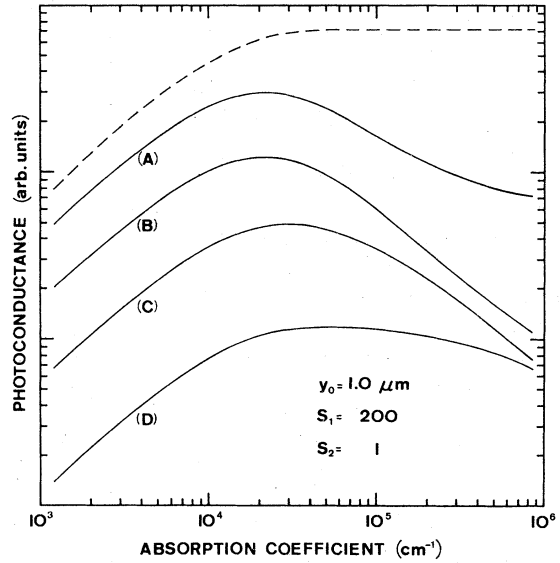


FIG. 2. Photoconductance vs absorption coefficient for 1.0- μm -thick specimen having $S_1=200$, $S_2=1$, and L^* equal to (A) 10^{-3} , (B) 10^{-4} , (C) 10^{-5} , and (D) 10^{-6} cm.

Such behavior is also illustrated in Fig. 3, which shows spectra for a 10.0- μm -thick specimen. Note that the photoconductance maxima are shifted to smaller values of α in this case, principally because of the increase in sample thickness.

In the strong absorption regime $\alpha Y_0 \gg 1$, in which case (1) reduces to

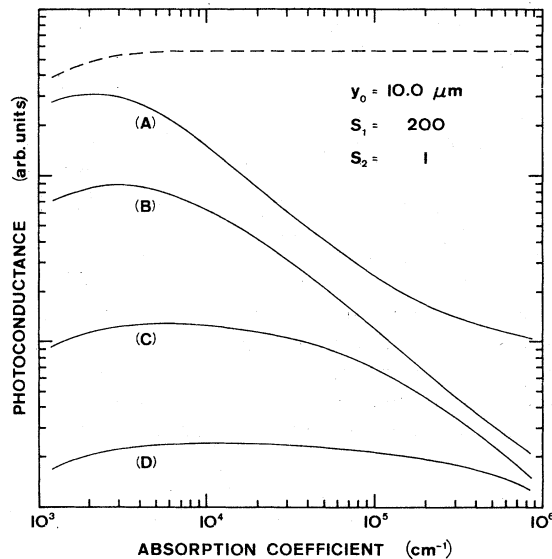


FIG. 3. Photoconductance vs absorption coefficient for 10.0- μm -thick specimen having $S_1=200$, $S_2=1$, and L^* equal to (A) 10^{-3} , (B) 10^{-4} , (C) 10^{-5} , and (D) 10^{-6} cm.

$$\Delta G = \Delta \sigma \left(\frac{1}{A} + \frac{(S_1 S_2 + A S_2)(1 - \cosh Y_0) - (S_1 + A) \sinh Y_0}{(S_1 S_2 + 1) \sinh Y_0 + (S_1 + S_2) \cosh Y_0} \right). \quad (5)$$

The strong absorption condition corresponds to carrier generation at the illuminated surface and in the bulk but not at the back surface. Note, however, that (5) contains S_2 as a parameter, which implies a continuing interaction with the surface at $y = y_0$. This interaction occurs because of carrier diffusion. However, if the specimen thickness is large compared to the diffusion length L^* , then $Y_0 \gg 1$ and $\sinh Y_0 \approx \cosh Y_0 \gg 1$. Under these conditions (5) reduces to

$$\Delta G(\lambda) = \frac{(1+K)^2}{2K} \frac{e^2 \beta I_0 L^{*2}}{kT} \frac{S_1 + A + 1}{(S_1 + 1)(A + 1)}, \quad (6)$$

where $\Delta G(\lambda)$ is the photoconductance under illumination at wavelength λ . Equation (6) can be used to obtain values for S_1 and L^* . The photoconductance ratios

$$R_{21} = \Delta G(\lambda_2) / \Delta G(\lambda_1), \quad R_{31} = \Delta G(\lambda_3) / \Delta G(\lambda_1) \quad (7)$$

give two equations involving these parameters and can be solved simultaneously. This procedure yields

$$L^* = \frac{(\alpha_1 - \alpha_2) R_{31} + (\alpha_3 - \alpha_1) R_{21} + (\alpha_2 - \alpha_3)}{\alpha_3(\alpha_2 - \alpha_1) R_{31} + \alpha_2(\alpha_1 - \alpha_3) R_{21} + \alpha_1(\alpha_3 - \alpha_2)}, \quad (8)$$

where α_1 , α_2 , and α_3 are absorption coefficients for λ_1 , λ_2 , and λ_3 , respectively. In addition, the front surface number S_1 is obtained as

$$S_1 = \frac{(1 + A_2)(1 + A_1)(1 - R_{21})}{(1 + A_2)R_{21} - (1 + A_1)}, \quad (9)$$

where $A_1 = \alpha_1 L^*$ and $A_2 = \alpha_2 L^*$. With these parameters determined, (6) then can be employed to obtain a value for $(1+K)^2/2K$, provided β is taken to be unity. This is ordinarily a good approximation in the strong absorption regime. Note, however, that one need only assume *constant* rather than unit quantum efficiency to obtain (8) and (9). A value for S_2 can be obtained by illuminating the specimen surface at $y = y_0$ and repeating the above procedure. In this way, all of the transport parameters which characterize the photogenerated electron-hole plasma can be determined.

Note that in doped materials the diffusion length³

$$L^* = \left(\frac{kT}{e} \frac{2K}{1+K} \mu_p \tau_p \right)^{1/2} = \left(\frac{kT}{e} \frac{2}{1+K} \mu_n \tau_n \right)^{1/2}, \quad (10)$$

which is the same for both types of carriers, is controlled by capture of the minority carrier,

whereas $\Delta \sigma$ reduces to

$$\Delta \sigma = e \beta I_0 \mu_m \tau_m [A / (1 - A^2)], \quad (11)$$

where the subscript m refers to the majority carrier. Thus the magnitude of the photoconductance may increase appreciably with doping, since τ_m does, even though the material may still be characterized by small L^* such that the photo-generated plasma is confined to a thin region at and near the illuminated surface. This phenomenon is fundamentally different from the trap-free lifetime case in which both types of photo-generated carriers have a common lifetime.

The above analysis applies to high-resistivity amorphous semiconductors which exhibit a photoconductance directly proportional to I_0 and provides a method for characterizing both surface and bulk properties of such materials. In particular, it provides a simple method for determining whether or not the very small diffusion lengths which have been predicted² for the amorphous state do indeed occur.

Other investigators⁷⁻¹¹ have interpreted photoconductivity in amorphous semiconductors using an equation of the form

$$\Delta G = e \beta \mu \tau I_0 (1 - e^{-\alpha y_0}), \quad (12)$$

where $\mu \tau$ is the carrier mobility-lifetime product. Equation (12) has been used, for example, in the analysis of *a*-Si:H films^{7,8} which exhibit photoconductance spectra of the type shown in Figs. 1 and 2. To account for the observed decrease in photoconductance in the strong absorption regime it has been suggested^{7,8} that $\beta \mu \tau$ varies in this region by as much as an order of magnitude. We wish to point out that (12) does not satisfy the usual surface boundary conditions except in the limit $S_1 = S_2 = 0$. This limit cannot be achieved even for specially prepared single-crystal surfaces and cannot be justified for the amorphous state. Here, the observed behavior is attributed to surface recombination processes in *a*-Si:H. Indeed, *the fact that the surface of this material may be modified such that $S_1 > 1$ is a direct indication of the high quality of the bulk.*

Equations (8) and (9) hold also for linear transport in lifetime semiconductors. For the trap-free case, the photoconductance is again given by (1), with

$$\Delta \sigma = e \beta I_0 (\mu_n + \mu_p) \tau [A / (1 - A^2)], \quad (13)$$

where τ is the excess carrier lifetime. In addition, $L^* = (D^* \tau)^{1/2}$, where D^* is the ambipolar diffusivity.¹² For the large diffusion lengths

which are typical of the lifetime case, (1) predicts a sharp peak in the photoconductance in the vicinity of the absorption edge. This is the observed behavior in many thick crystalline semiconductors.¹³

ACKNOWLEDGMENT

This work was supported by the National Science Foundation under Grant No. DMR 77-08443.

¹W. van Roosbroeck and H. C. Casey, Jr., Phys. Rev. B 5, 2154 (1972).

²W. van Roosbroeck, J. Non-Cryst. Solids 12, 232 (1973).

³J. F. Schetzina, Phys. Rev. B 11, 4994 (1975).

⁴J. F. Schetzina, Phys. Rev. B 12, 3339 (1975).

⁵M. Hegems and H. J. Queisser, Phys. Rev. B 12, 1443 (1975).

⁶H. B. DeVore, Phys. Rev. 102, 86 (1956).

⁷R. J. Loveland, W. E. Spear, and A. Al-Sharbaty, J. Non-Cryst. Solids 13, 55 (1973).

⁸P. J. Zanzucchi, C. R. Wronski, and D. E. Carlson,

J. Appl. Phys. 48, 5227 (1977).

⁹T. D. Moustakas, D. A. Anderson, and W. Paul, Solid State Commun. 23, 155 (1977).

¹⁰H. Fritzsche, C. C. Tsai, and P. Parsons, Solid State Technol. 21, 55 (1978).

¹¹N. F. Mott and E. A. Davis, *Electronic Processes in Non-Crystalline Materials* (Clarendon, Oxford, 1971).

¹²R. M. Shah and J. F. Schetzina, Phys. Rev. B 5, 4014 (1972).

¹³R. H. Bube, *Photoconductivity of Solids* (Wiley, New York, 1960).